"AUTO-OSCILLATION OF CAVITATING INDUCERS"

D.M. BRAISTED + C.E. BRENNEN

PAPER IN :

Polyphase Flow and Transport Technology

presented at

THE SYMPOSIUM ON POLYPHASE FLOW AND TRANSPORT TECHNOLOGY
CENTURY 2 — EMERGING TECHNOLOGY CONFERENCES
SAN FRANCISCO, CALIFORNIA
AUGUST 13-15, 1980

sponsored by

THE FLUIDS ENGINEERING DIVISION, ASME

edited by

R. A. BAJURA
WEST VIRGINIA UNIVERSITY

THE AMERICAN SOCIETY OF MECHANICAL ENGINEERS
United Engineering Center 345 East 47th Street New York, N.Y. 10017

AUTO-OSCILLATION OF CAVITATING INDUCERS

D. M. Braisted and C. E. Brennen
California Institute of Technology
Pasadena, California

ABSTRACT

This paper presents details of measurements on the instability known as auto-oscillation which occurs in systems with cavitating pumps. Specific measurements are made of onset cavitation number and auto-oscillation frequency for a range of inducers. It has been shown that auto-oscillation is a system instability caused by the active dynamic characteristics of the cavitating pump.

A system analysis is presented which utilizes previously measured dynamic transfer functions for the inducers; the resulting predictions of instability are consistent with the observations. Though the onset cavitation number is a function of the entire system it is also shown that, given the onset cavitation number, the auto-oscillation frequency is only weakly dependent on the system and primarily a function of the pump dynamics.

Detailed measurements of the amplitude and phase of fluctuating pressures and flow rates during auto-oscillation are also presented. These strongly suggest that the pump dynamics are primarily determined by the complicated flow at inlet to the inducer which involves pre-swirl generated by a strong backflow. Some data on the non-linear effect of auto-oscillation on overall mean performance are also presented.

Nomenclature

A	Inducer inlet area
a_{ijk}	Polynomial coefficients for transfer function jets
C	Air bladder compliance
ΔE	Fluctuating energy drain of system
Δe	$\Delta E/\lvert\tilde{h}_1\rvert^2$
H	Blade tip spacing = circumference/number of blades
$\bar{h}$	Mean total head
$\tilde{h}$	Fluctuating total head
I_u, I_D	System impedances upstream and downstream of pump
$\bar{m}$	Mean mass flow rate
$\tilde{m}$	Fluctuating mass flow rate
$[S]$	System transfer function
$[T]$	Transfer function
U_T	Impeller tip speed
$[Z]$	Pump transfer function
φ	Flow coefficient = Pump Flow Rate/AU_T
ψ	Head coefficient = Head rise across pump/ρU_T^2
σ	Cavitation number = Net positive suction pressure/ $\frac{1}{2}\rho U_T^2$
ρ	Liquid density
Ω	Radian frequency
ω	Reduced frequency = $\Omega H/U_T$
ω_N	Natural reduced frequency
$[I]$	Identity matrix

1. INTRODUCTION

The phenomenon of auto-oscillation or surge has often been encountered with cavitating pumps (for example Refs. [1] to [14]). It represents one of the commonest instabilities derived from two phase flow which are encountered in hydraulic systems. It can be quite deleterious to the operation, performance, control and lifetime of a pump.

In this paper we present an account of experimental investigation of auto-oscillation in cavitating inducers and attempt to correlate these observations with a model for hydraulic system analysis based on recent improvements in the state of knowledge of the unsteady, dynamic characteristics of cavitating pumps (for more detail see [15]). We shall concentrate on auto-oscillation and make only passing reference to the less severe instabilities such as rotating cavitation and alternate blade cavitation [3,4,6,7] which can sometimes occur in inducers. These are probably less troublesome because they are local flow oscillations in which the rest of the hydraulic system does not usually become excited. Furthermore, we shall not consider the added complications which arise when the inlet and discharge lines become sufficiently long for acoustic resonance frequencies in these lines to be excited by blade passage frequencies [16]. Such phenomena could however be accommodated by the inclusion of compressible pipe flow transfer functions (see Ref. [17]) in the stability analysis rather than the incompressible models used in Section 7. Finally, we shall consider only hydraulic systems which are fixed in some non-inertial coordinate system. The methodology could clearly be expanded for the analysis of accelerating systems such as occur in the POGO instability in liquid propelled rockets [18,19,20]. However, this requires a stipulation of the interaction between the global acceleration of the unsteady flow rate relative to the system which is beyond the scope of the present paper.

Auto-oscillation is a function of the entire

hydraulic system of which the cavitating pump may be only a small part. It has been recognized [1,5,7,12, 13,14] that the system influences the onset and amplitude (and perhaps the frequency) of the oscillation but that the cavitation in the pump is the source of the problem. There exists a number of speculations [3,4,6,10,13,14] on the precise mechanism through which the cavitation excites and sustains the instability but none are proven. Both Barr [4] and Etter [6] suggest that it is associated with an inherent instability in the cavity length when this is close to the blade passage length [4] or when the cavity on one blade collapses at the entrance to the next blade passage [6]. Badowski [3] has proposed an instability in the coupling between the cavitation, the head production and the backflow induced prerotation. Both Sack and Nottage [13] and Young, Murphy and Reddecliff [14] have attempted to factor in system effects though their analyses are limited by lack of information on the dynamic characteristics of cavitating inducers. The recent availability of dynamic transfer functions for cavitating inducers [21,11,12,22,23,24] has permitted a more accurate evaluation of such system effects.

Finally, we should comment on the evident analogy between auto-oscillation and the surge phenomena which occurs in compressors [25,26]. (We note in passing that rotating cavitating and rotating stall also appear to be superficially analogous.) The major difference is that the cavitating pump instabilities can occur at operating points where the slope of the head rise versus flow rate curve is negative. On the other hand, Greitzer [25] has indicated that a positive slope is necessary for the compressor instabilities. In the case of surge he concisely describes the need for a minimum positive slope in order to provide a source of fluctuating energy sufficient to overcome the dissipation in other parts of the system. The analysis of Section 7 similarly defines such a minimum for pumps in the absence of cavitation.

Similar instabilities in regions of positive head rise/flow rate slope can occur with cavitating or non-cavitating pumps [27]. However, auto-oscillating usually occurs in regions of negative slope when the extent of cavitation has reached some critical value. Therefore, it is evident that cavitation has the potential of providing some other source of fluctuating energy different from that in the compressor problem. Indeed cavitation-induced auto-oscillation occurs when the system is apparently stable according to the kind of quasi-static analysis used in the compressor problem. In the present paper we attempt to demonstrate that auto-oscillation is due to the dynamic rather than the quasi-static characteristics of the cavitating pumps. We feel that similar attention should be paid to the dynamic as opposed to the quasi-static behavior of compressors. Indeed Ng and Brennen [12] found that the characteristics deviated substantially from quasi-static values for reduced frequencies based on tip speed and circumferential blade spacing as low as 0.1.

2. EXPERIMENTAL FACILITY

The experimental investigation of auto-oscillation was performed in the Dynamic Pump Test Facility (DPTF) at the California Institute of Technology; a schematic of this facility which is described elsewhere [11,12,15] appears as Fig. 1. Instrumentation utilized in the experiments include (i) two laser

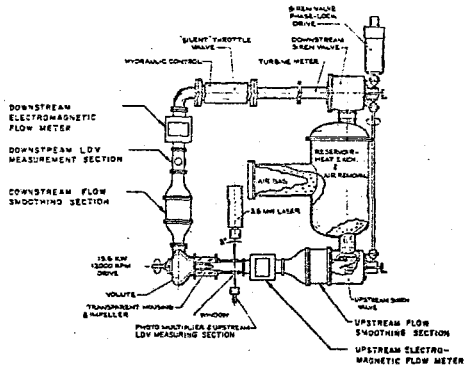

Fig. 1 Schematic plan view of the Dynamic Pump Test Facility used in present experiments.

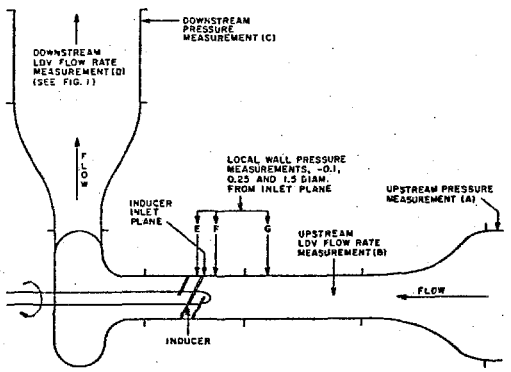

Fig.2 Schematic showing pressure and flow rate measurement locations. Transducers were also placed at various circumferential locations at the points E and F. Letters are used for presentation of results in Fig. 7,8 and 9.

doppler velocimeters for measurement of the unsteady flow rate at inlet to and discharge from the pump (ii) two strain gauge pressure transducers for measurement of the total head fluctuations of the inlet and discharge flows (iii) variable reluctance transducers mounted on the wall of the duct in the neighborhood of the inlet to the transducer so as to determine the axial and circumferential variations in fluctuating pressure in this region (axial locations are indicated in Fig. 2). All of this dynamic data was recorded simultaneously on a 14-channel Ampex tape recorder and processed using a Spectral Dynamics signal analyzer in order to obtain spectra and cross-correlations. Additional instrumentation included a turbine flow meter and a magnet proximity transducer to monitor the rotational speed.

Experiments were performed using five different inducer/impellers. Impellers 4 and 6 were 7.6cm. and 10.26cm. diameter models of the low pressure oxygen pump rotors in the Space Shuttle main engine [12]. Impellers 5 and 7 are geometrically similar 7.6cm. and 10.26cm. diameter three-bladed helical impellers with swept leading edges, zero blade cant and 9° blade angle [1]. Impeller 8 was 10.26 cm.diameter four-bladed helical inducer with a zero blade cant, swept

leading edges and a 7 1/2° blade angle. Impellers 5, 7,8 had a solidity of 2.

The major role played in auto-oscillation by the swirling inlet flow and the cavitating backflow (see below) suggested conducting experiments with sections of honeycomb installed in the inlet line in order to partially suppress the prerotation. This honeycomb section was 2.5cm. long and, when installed, was located so that it was about 2 diameters upstream of the inlet to the 10.2cm. inducers.

3. PRELIMINARY OBSERVATIONS

All inducers exhibited auto-oscillation to some degree as the prevailing pressure level was reduced. In general onset (see Sections 4 and 5) occurred at cavitation numbers for which there was extensive inducer cavitation but for which there was little or no degradation of performance. Typical onset points are shown in the cavitation performance graph for Impeller 6 included as Fig. 3 (the non-cavitating performance of this inducer was included in Ref. [22]). With further reduction in pressure the auto-oscillation seemed to decline as the head breakdown proceeded; a rough indication of desinence is also included in Fig. 3. Both of these features of auto-oscillation have been noted previously [7,14]. However, the decrease in the onset cavitation number with decreasing flow coefficient is not a feature which is universally observed.

Kamijo et al [7] reported that a rotating cavitation instability seemed to occur for a range of σ adjacent to but larger than the auto-oscillation range for their inducers. Occasional but unrepeatable observations of rotating cavitation were made during the present experiments in a similar range of σ. However, these occurred only with Impeller 4 and 6 and were so rare and ephemeral that they will not be discussed further. Some similar occasional observations of alternate blade cavitation were made for Impellers 7 and 8.

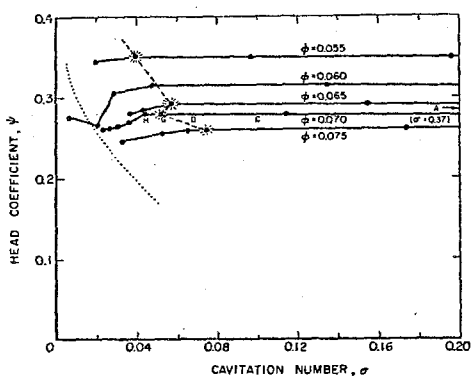

Fig. 3 Cavitation performance of Impeller 6 at five flow coefficients, φ, as indicated. Onset (—☼—) and approximate desinence (·····) boundaries of auto-oscillation region for 6000 rpm are indicated. Letters refer to conditions for which transfer functions are available [22]. Uncertainties are about ± 0.002 in ordinate and abscissa.

Visual observations clearly showed that the cavitating backflow generated by the tip clearance flow oscillated violently during auto-oscillation and that both the backflow and auto-oscillation disappeared together with decrease in pressure through breakdown. This suggests that the inlet flow field of which the backflow is an integral part plays a major role in the inducer dynamics and the auto-oscillation phenomenon. Consequently, wedge probe and total head probe surveys were made of the inlet flow field in order to document the mean flow velocity profiles of the inlet flow. These measurements were made with a manometer so that any time dependence or three-dimensional turbulent structures in the flow were averaged out. Typical mean axial and swirl velocity profiles calculated under the assumption of radial equilibrium are presented in Figs. 4 and 5 for an axial location 0.25 diameters upstream of the inlet plane of impeller 6; data is shown with and without the section of

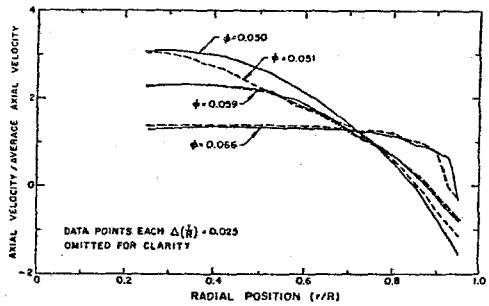

Fig. 4 Axial velocity profiles 0.25 diameters upstream of inducer inlet plane for Impeller 6 at various flow coefficients, φ, and with (————) and without (- - - - -) honeycomb section. Based on radial equilibrium assumption. Uncertainty is about ± 0.05 on ordinate.

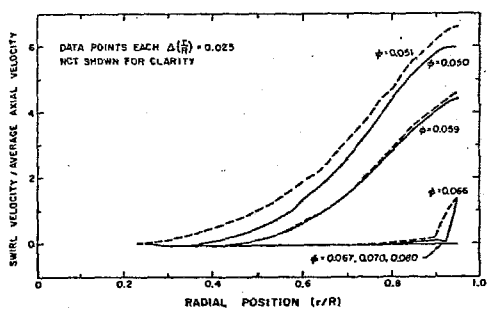

Fig. 5 Swirl velocities corresponding to Fig. 4. Uncertainty is about ± 0.1 on ordinate.

honeycomb in the inlet line. Figure 4 shows that a region of reversed flow or backflow occurs at this location and increases in extent (as well as upstream penetration distance) as the flow coefficient decreases. This is clearly due to the increasing head rise across the pump which drives the tip-clearance flow and backflow. The swirl velocity profiles shown in Fig. 5 show zero swirl in the absence of backflow ($\varphi > 0.066$ for this location). The swirl (or prerotation) increases dramatically as the backflow increases. Profiles obtained at 6000 rpm and at 4000 rpm were essentially identical. Profiles from measurements made 0.5 diameters and 2.8 diameters upstream revealed reduced perturbations and zero perturbation to a uniform, non-swirling inlet flow. At the 0.5 diameter location no swirl velocities were observed for $\varphi > 0.063$. The above were all obtained under non-cavitating conditions; despite difficulties in repeating the data under cavitating conditions due to

bubble formation in the manometer lines some limited measurements at $\sigma \approx 0.1$ indicated similar profiles to those without cavitation.

These inlet velocity profiles which are similar to those observed by Rosenmann [28,29] deserve further comments. It is clear that swirl (or circulation) only occurs in the presence of backflow, thus it satisfies Kelvin's theorem since far upstream the flow has zero circulation and consequently the backflow must be entirely responsible for the swirl. However, it is also clear that the circulation which is induced by the backflow is not confined to the reversed flow. Furthermore, any simple estimate of the radially inward diffusion of circulation due to laminar viscous effects forces one to conclude that such diffusion is much too small to account for the circulation observed in the core of the flow. Evidently some large unsteady turbulent structures must be present which transport vorticity to the core. These fluid phenomena which will be addressed in a later paper are, we feel, important to the performance of a turbomachine; they deserve closer inspection than they have been given in the past.

4. AUTO-OSCILLATION FREQUENCY

At high cavitation numbers the low level pressure and mass flow rate fluctuations were random with a broad frequency spectrum [15]. When the cavitation number was reduced the onset of auto-oscillation was characterized by a dramatic increase in the level of pressure and mass flow rate fluctuation in the system (see Figs. 7 and 8); it was also clear visually and audibly. The spectra of the pressure and flow rate fluctuations then contained a dominant frequency [15] which we define as the "auto-oscillation frequency". These auto-oscillation frequencies will be presented as a reduced frequency, ω, based on the blade tip spacing and the tip velocity. The reduced auto-oscillation frequency for a given inducer was found to depend on a number of factors including the impeller rotating speed, the flow coefficient, φ, and the cavitating number, σ. However, preliminary tests clearly demonstrated that for a given φ and σ the reduced frequency was virtually independent of rotating speed at least in the range 4000 → 7000 rpm [15]. In other words, the actual frequency was linearly proportional to the rotating speed. This is consistent with the results of other studies such as those in reference [10].

Some typical variations in the reduced auto-oscillation frequency, ω, with φ and σ are presented in Fig. 6. Almost all of the data suggests a monotonic decrease in ω with decreasing cavitation number, a trend which has been noted by other investigators [3,9,10,14] and by Acosta and Wade [30] in their studies of cavitating cascade instabilities. Indeed the frequencies given by Young, Murphy and Reddecliff [14] present a very similar picture to those in Fig. 6 not only qualitatively but also quantitatively.

The data for Impeller 6 in Fig. 6 also shows some increase in ω with increasing flow coefficient, a trend which was also demonstrated by running tests for fixed σ and varying φ [5]. Also included in Fig. 6 are frequencies manifest by Impeller 7 with and without the section of honeycomb inserted in the inlet line. The increased frequencies caused by the honeycomb are consistent with the claim made earlier

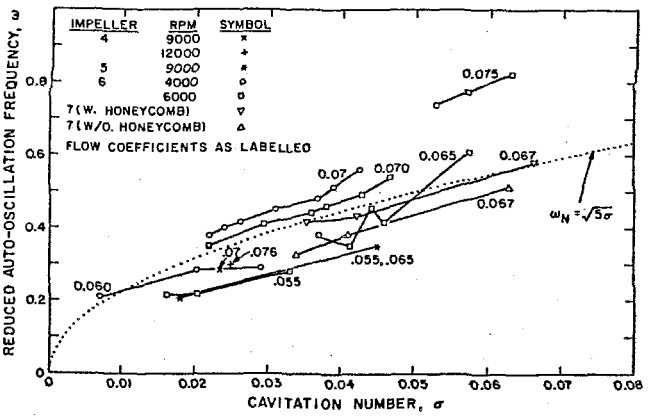

Fig. 6 *Reduced auto-oscillation frequencies plotted* against cavitation number for different impellers and rotating speeds. Also shown is the estimated "natural frequency" $\omega_N = \sqrt{5\sigma}$. Uncertainities are about ± 0.002 on abscissa, ± 1% on ordinate.

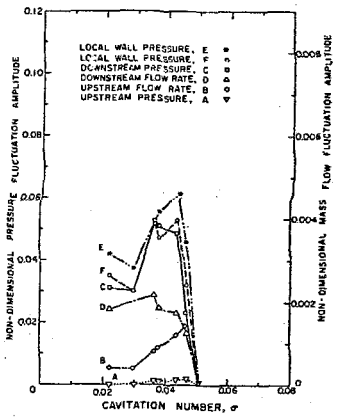

Fig. 7 Non-dimensional amplitudes of fluctuating pressure and mass flow rate plotted against cavitation number for Impeller 6 at $\varphi = 0.07$ and 6000 rpm. Uncertainties are about ± 0.002 on abscissa, ± 5% on ordinate.

in the context of the swirl observations, namely that the honeycomb simply increases the "effective" flow coefficient.

It is instructive to compare the reduced auto-oscillation frequencies for the two sets of geometrically similar inducers, Impellers 5 and 7 and Impellers 4 and 6. Only limited data was obtained for Impeller 4 but reduced frequencies were about 0.29 at both 9000 and 12000 rpm for $\sigma \approx 0.025$, $\varphi = 0.07$; these are consistent with the reduced frequencies for Impeller 6 though the onset cavitation is quite different for comparable flow coefficients. Some data for Impeller 5 is also shown in Fig. 6. Again the reduced frequencies are comparable with those for Impeller 7 though the onset cavitation numbers differ substantially.

One of the points to be made in the present paper is that auto-oscillation is an instability of the entire hydraulic system. The above data suggests that though the onset does indeed appear to depend strongly

on the system, the reduced frequency of the instability appears to be primarily determined by the dynamics of the inducer alone. One might therefore ask whether the frequency of auto-oscillation for a particular inducer operating under given conditions φ, σ could be predicted from knowledge of the transfer function of the inducer alone without reference to the rest of the system. Such a prediction does not clearly emerge from the stability analysis presented later in Section 7. However, a much simpler heuristic model does produce surprising agreement with the experiments (Fig. 6). If the cavitating inducer has an inherent natural frequency, then it seems likely that this is derived from the inertance and compliance of the inducer pump acting as a mass and spring respectively. In the experiments the inertance of the pump is much larger than the inertance of the rest of the hydraulic system; this would help explain the lack of sensitivity of the auto-oscillation frequency to the rest of the system. To proceed we therefore take non-dimensional pump inertances and compliances ($-a_{112}$ and $-a_{121}$) from Figs. 11 and 12 of Ref. [22]. The former is very roughly constant at a value of about 40 whereas the latter varies with the cavitation number like $0.005/\sigma$. On this basis the reduced natural frequency of the inducer would be $\omega \approx \sqrt{5\sigma}$ where possible variations with φ have been neglected. This "natural frequency" is shown in Fig. 6. It is in remarkably good agreement with the "auto-oscillation" frequencies which suggests that such a heuristic model has some validity.

However, it is clear that in some practical systems with long inlet or discharge lines the inertance of these lines may not be small compared with the pump inertance. Under such circumstances it seems reasonable to suggest that the total system inertance rather than simply the pump inertance should be used in estimating the auto-oscillation frequency.

5. AUTO-OSCILLATION AMPLITUDES AND PHASE RELATIONSHIPS

The amplitudes of the pressure and mass flow rate fluctuations at the auto-oscillation frequencies were obtained as the magnitude of the peaks in the spectra. Following application of the frequency dependent signal processor calibrations and the transducer calibrations (see Ref. [15] for pressure transducer calibrations) the magnitudes of the pressure and mass flow rate fluctuations were non-dimensionalized by ρU_T^2 and $\rho A U_T$ respectively. Some examples of the variation in the fluctuation amplitudes with the operating conditions are shown in Figs. 7 and 8. These all show the dramatic onset at a particular cavitation number as σ is reduced. With further reduction in σ the oscillations reach a peak and subsequently decline. Note that the amplitudes of the actual fluctuations are large reaching 50 psi in pressure and 20% of the mean flow rate.

More specifically Fig. 7 presents the data for Impeller 6 at a rotating speed of 6000 rpm and $\varphi = 0.07$. Figure 8 demonstrates a typical variation with flow coefficient for Impeller 6. Other data is included in Ref. [15]. Figure 7 indicates that virtually all pressure and flow rate measurements behave in a similar manner; Fig. 8 shows that the onset and maximum amplitude varies considerably with the flow coefficient. The onset and disappearance points for this case were plotted in Fig. 3. It should be stressed that the disappearance seemed to correspond with

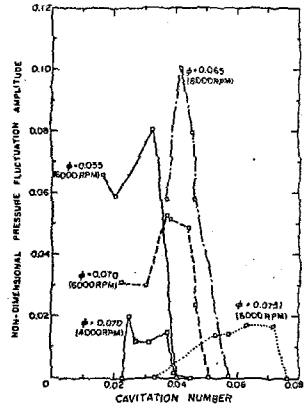

Fig. 8 Non-dimensional amplitudes of fluctuating downstream pressure (C) for Impeller 6 at various flow coefficients and rotating speeds. Uncertainities and are about ±0.002 on abscissa, ±5% on ordinate.

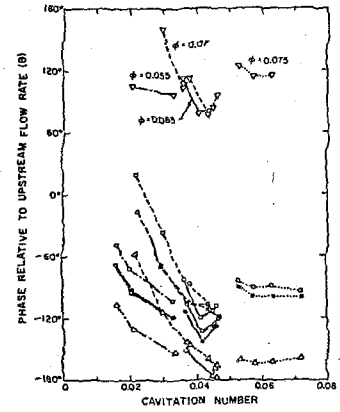

Fig. 9 Phase of the fluctuating quantities relative to the oscillations in the upstream flow rate (B) for various flow coefficients; φ=0.055: —·—; φ=0.065: ——— ; φ = 0.070: - - - -; φ = 0.075; · · · · Phase shown for upstream pressure, A(▽), downstream pressure, C(□), local pressure, E and F(* and O) and downstream flow rate, D(Δ), as in Fig. 7. Uncertainities are about ±0.002 on abscissa, ±5° on the ordinate.

visual observations of the disappearance of cavitating backflow which is associated with the breakdown of the inducer.

Some further insight into the phenomenon can be gained by considering typical amplitude data as represented by Fig. 7 in conjunction with the corresponding data on the relative phases of the fluctuations presented in Fig. 9. These phases were obtained by cross-correlation using the spectrum analyzer. The upstream flow rate has been arbitrarily chosen as the phase reference in the presentation of the data.

Several characteristics of the phase relationships should be noted. First observe that though the phase of a particular measurement is a function of both φ and σ there is a qualitatively consistent phase relationship between any two fluctuating quantities. For example, the downstream flow rate generally lags behind the upstream flow rate by about 160° whereas the upstream pressure generally leads it by

about 110°. On closer inspection one can also observe that there are fairly consistent changes in the phases as the cavitation number is reduced: for example, the phase by which the downstream pressure lags the upstream flow rate decreases with σ. It should however be emphasized that since the instability is a function not only of the pump but also of the entire system of which the pump is one part, it follows that these relationships are also a function of the entire hydraulic system.

There is however one intriging feature of these results which appears to be directly connected with the pump dynamics. First, note from Fig. 7 that the amplitudes of the pressures measured in the vicinity of the inlet plane of the inducer are much larger than those of the upstream pressure oscillations; this is true even for the wall pressure 0.25 diameters upstream of the inlet plane (Figs. 2 and 7). Secondly, one can see from Fig. 9 that these wall pressures near inlet are almost in-phase with the downstream pressure for all cases tested; on the other hand, the phase relative to the upstream pressure is large and variable.

Only the phase for a single inlet region wall pressure is shown in Fig. 9. Cross-correlation revealed negligible phase differences between wall pressures measured either at the three axial locations shown in Fig. 2 or at several circumferential locations at one axial location.

These facts all suggest that the wall pressure measurements characterize the tip clearance flow and backflow jet and that these are closely coupled to the conditions downstream of the pump. Note, for example, from the axial and swirl velocity profiles in Figs. 4 and 5 that the backflow extends more than 0.25 diameters upstream for $\varphi < 0.067$. The data for $\varphi > 0.067$ suggests the influence of the backflow extends further upstream than the jet itself penetrates. Thus, in summary, it appears that the dynamics of the inlet flow and the backflow jet contribute in a major way to and is an integral part of the dynamics of the pump.

6. NON-LINEAR EFFECTS

In the following sections a linear perturbation model is proposed whose purpose is the prediction of the onset cavitation number and frequency of auto-oscillation. It is however clear that such a model cannot predict the amplitude reached when the system is operated under unstable conditions. This would ultimately require detailed knowledge of the non-linear dynamic behavior of the cavitating inducer and the rest of the hydraulic system. At the present time such knowledge is very limited. Consequently, we conclude the account of the experimental observations with a description of some of the non-linear effects which were observed.

The most notable non-linear effect manifest during operation within the unstable region was the effect upon the mean flow through the inducer. This effect varied greatly from one impeller to another. Impeller 8 displayed a large reduction in mean flow performance as shown in Fig. 10. There was, moreover, a hysteretic character to this non-linear effect as indicated in the figure. As the cavitation number was reduced and the auto-oscillation began, there was a large decrease of the order of 50% in the head developed. The shift in σ associated with this head loss which is shown in Fig. 10 is in part due to a lack of ability to control both φ and σ during this transient. If one then attempted to reverse the process by increasing σ in order to get out of the auto-oscillation the path followed is different as indicated in the figure and this produces the hysteretic behavior. In some ways this hysteretic behavior resembles that encountered in compressor surge [25]. Incidentally,

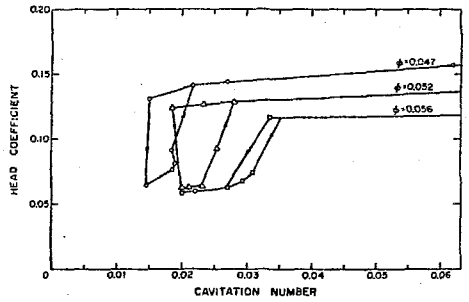

Fig.10 Non-linear hysteretic behavior of Impeller 8 at three flow coefficients as labelled. Uncertainty is ±0.002 on abscissa and ordinate.

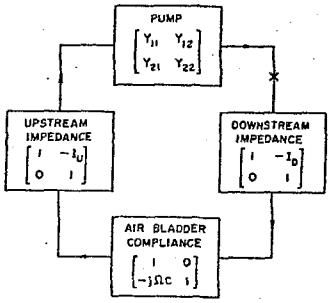

Fig. 11 Schematic of dynamic model used to analyze the stability of the Dynamic Pump Test facility.

it is curious that the head developed during auto-oscillation is essentially the same for each of the three flow coefficients. The non-linear head loss associated with Impeller 6 was much smaller in magnitude for reasons which are not clear.

7. LINEAR DYNAMIC MODEL FOR AUTO-OSCILLATION ONSET

In this section, we shall construct a linear dynamic model of the hydraulic system whose object will be the prediction of the onset of auto-oscillation. The key here is the form of the dynamic model which must be used to represent the dynamic behavior of the cavitating inducer. Fanelli, [31], Brown [32], Brennen and Acosta [21] and others have proposed that such linear problems are more readily handled in the frequency domain. The instantaneous total head and mass flow rate at each point in the hydraulic system are divided into mean components, $\bar{h}$ and $\bar{m}$, and fluctuating components at each frequency, Ω, represented as the real parts of $\tilde{h}e^{j\Omega t}$ and $\tilde{m}e^{j\Omega t}$ where $\tilde{h}$ and $\tilde{m}$ are complex to represent the phase relationships of the fluctuating quantities. Then the dynamic behavior of the hydraulic system between any two points denoted by subscripts 1 and 2 (where

1 normally denotes the inlet and 2 the discharge point) can be represented by a transfer matrix, [T],

$$\begin{Bmatrix} \tilde{h}_2 \\ \tilde{m}_2 \end{Bmatrix} = \begin{bmatrix} T_{11} & T_{12} \\ T_{21} & T_{22} \end{bmatrix} \begin{Bmatrix} \tilde{h}_1 \\ \tilde{m}_1 \end{Bmatrix} . \qquad (1)$$

The transfer matrix will be a function not only of frequency, Ω, but also of the mean flow conditions. For a straight pipe or accumulator, for example, one can anticipate the form of [T] with some confidence. However, for a more complex flow such as that through a cavitating inducer this is not so easily done. Recently, transfer functions for cavitating inducers have been measured [11, 12, 22] and compared with a theoretical model [23,22] for a number of inducers over a range of frequencies, cavitation numbers and flow coefficients. These studies have shown that an inducer becomes an increasingly "active" dynamic device [33] as the extent of cavitation within it increases. Consequently, the inducer provides the source of the fluctuating energy production necessary to overcome the frictional dissipation normally associated with the inlet and discharge lines and to sustain the auto-oscillation. It is therefore essential in any predictive model to properly represent the inducer by an active transfer function which we will denote by [Z] ([Z] = [Y]-[I] see (Fig. 11)). Here we will simply use the experimental transfer functions presented as functions of Ω, σ and φ in Refs. [12] and [22],

To complete the model, transfer functions for the rest of the closed loop system used in the experiments are needed. For this purpose it was assumed that the pump inlet line between the discharge from the large reservoir and the inducer inlet (Fig. 1) and the pump discharge line between the volute discharge and the reservoir inlet could both be represented by complex impedances as indicated in Fig. 11. These impedances were measured experimentally and conformed with expectation in terms of the resistance and inertial components [15]. Finally, it was assumed and confirmed by experiment [15] that the reservoir and the large air bag within it could be represented by a simple compliance, C, as shown in Fig. 11.

A convenient way in which to evaluate the stability of a closed loop system such as that represented by Fig. 11 is to "open" the circuit at some point. For convenience, a break-point just downstream of the pump is chosen (X in Fig. 11); it is clear that the final conclusions should be and are independent of the location of the break-point. Then the transfer matrix relating the conditions just upstream of the break (subscript 2) to those just downstream of the break (subscript 1) is [S] where

$$\begin{aligned} S_{11} &= 1+Z_{11} - j\Omega C[Z_{12}-I_U(1+Z_{11})] \\ S_{12} &= Z_{12}-(I_U+I_D)(1+Z_{11})+j\Omega C[I_D Z_{12}-I_U I_D(1+Z_{11})] \\ S_{21} &= Z_{21} - j\Omega C(1+Z_{22}-I_U Z_{21}) \qquad (2) \\ S_{22} &= 1+Z_{22} -(I_U+I_D)Z_{21}+j\Omega C[I_D(1+Z_{22}) - I_U I_D Z_{21}] \end{aligned}$$

Stability will be assessed on the basis on an energy flux criterion. The net flux of fluctuation energy entering the "opened" system at the break point is given by ΔE where, for convenience, this has been non-dimensionalized by $\rho U_T^3 A$:

$$\Delta E = \frac{1}{4}\{\bar{\tilde{m}}_1\tilde{h}_1 + \tilde{m}_1\bar{\tilde{h}}_1 - \bar{\tilde{m}}_2\tilde{h}_2 - \tilde{m}_2\bar{\tilde{h}}_2\} \qquad (3)$$

where an overbar denotes the complex conjugate. Substituting from the overall transfer matrix and equating $\tilde{m}_1 = \tilde{m}_2$ leads to

$$\Delta E = \frac{|\tilde{h}_1|^2}{2} \text{ Real } \{FG\} \qquad (4)$$

where

$$F = \frac{2A}{U_T} \frac{[Z_{21}+j\Omega C(I_U Z_{21}-1-Z_{22})]}{[Z_{21}(I_U+I_D)-Z_{22}+j\Omega C(I_U Z_{21}-1-Z_{22})]} \qquad (5)$$

$$G = \frac{Z_{11}Z_{22}+Z_{21}A_1+j\Omega CA_2}{Z_{21}(I_U+I_D)-Z_{22}+j\Omega CA_3}$$

where

$$\begin{aligned} A_1 &= I_U+I_D-Z_{12} \\ A_2 &= Z_{12}+I_U I_D Z_{21}-I_U(1+Z_{11})-I_D(1+Z_{22}) \end{aligned}$$

and

$$A_3 = I_U Z_{21}-1-Z_{22} \ . \qquad (6)$$

These expressions are greatly simplified by observing that the compliance C in the experiments is very large in magnitude and the terms involving C dominate the numerators and denomiator. Hence

$$\Delta E \approx \frac{|\tilde{h}_1|^2}{2} \text{ Real } \left[\frac{I_U(1+Z_{11})+I_D(1+Z_{22})-Z_{12}-I_U I_D Z_{21}}{1+Z_{22}-I_U Z_{21}}\right] . \qquad (7)$$

Consequently the criterion for stability is as follows. If ΔE as evaluated using the above expression is positive then a flux of fluctuating energy must be supplied to the system at the break point in order to sustain the fluctuations. Hence if $\Delta E > 0$ the system is stable. If, on the other hand, $\Delta E < 0$ then the internal supply of fluctuating energy from the cavitating inducer exceeds the internal dissipation and the system is unstable. Several simple limiting cases are instructive. If the pump is not cavitating and one neglects fluid and structural compliance then $Z_{11} = Z_{21} = Z_{22} = 0$ [21]. In this case the stability depends entirely on the sign of $\text{Re}(I_U+I_D-Z_{12})$; that is to say on the magnitude of the total system resistance. The quasi-static pump resistance which is equal to $\text{Re}\{-Z_{12}\}$ as $\Omega \to 0$ is directly related to the slope of the steady state performance characteristic (Ψ versus φ). Since the quasi-static line resistances, $\text{Re}(I_U)$ and $\text{Re}(I_D)$, are positive it follows that if this slope is negative the system will inevitable be stable at low frequencies. If on the other hand, the slope is sufficiently positive the system may become unstable; such occurrences are well known [34,35,25,26,27]. It would however be wise to point out that all of the resistances are frequency dependent to some degree [12,15]. Consequently it is still possible for a

system to be stable to low frequencies but unstable in some higher range of frequencies even when the slope of the steady state characteristic is negative.

It is clear that when the inducer is cavitating so the Z_{11}, Z_{21} and Z_{22} are not necessarily zero then the condition for stability is less obvious and requires evaluation of the expression (7) containing characteristics not just of the pump but of the entire system.

8. RESULTS OF STABILITY CALCULATION

The methodology described in the last section can be readily modified for use in any hydraulic system. However, we concentrate on its use for predictions of auto-oscillation in the present experimental configuration. Values of $\Delta e = \Delta E/|\hat{H}_1|^2$ were calculated using Eq. (7) and each of the experimentally obtained pump transfer functions [Z], described in Refs. [12] and [22]. The latter were obtained for particular mean flow conditions, φ and σ, which imply a particular quasi-static system resistance external to the pump. This resistance could however be variously distributed between the inlet and discharge lines without changing the mean flow conditions. However, such redistribution can effect the system stability as suggested by the form of the expression (7) and as shown in Ref. [15].

The effect of changing the cavitation number, σ, while maintaining a fixed combination of system impedances is demonstrated in Fig. 12 for Impeller 4 (using six of the pump transfer functions labelled A to F which are presented

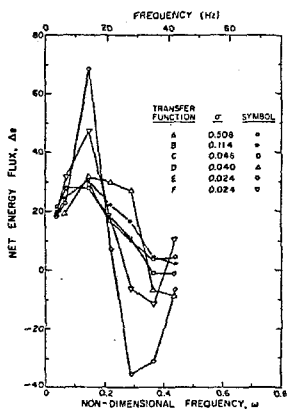

Fig. 12 The net energy flux, Δe, as a function of frequency for six cavitation numbers at which transfer functions (A to F) were obtained for Impeller 4 (at $\varphi = 0.07$ and 9000 rpm). Uncertainty in σ is $\pm$ 0.002; in Δe it increases from about $\pm$ 1 at lower frequencies to about $\pm$ 5 at higher frequencies.

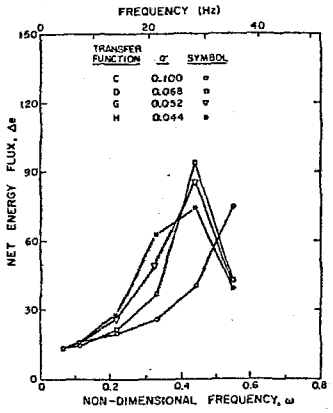

Fig. 13 The net energy flux, Δe, as a function of frequency for four cavitation numbers at which transfer functions (C,D,G,H) were obtained for Impeller 6 (at $\varphi \approx 0.07$ and 6000 rpm). Uncertainty in σ is $\pm$ 0.002; in Δe is increases from about $\pm$ 1 at lower frequencies to about $\pm$ 5 at higher frequencies.

in Ref. [12]) and in Fig. 13 for Impeller 6(using transfer functions labelled C,D,G,H which are presented in Ref. [22]). The combination of system impedances which were used were those measured for the conditions under which the auto-oscillation experiments were performed. Figure 12 indicates that with the 3 in. diameter Impeller 4 the system at $\varphi = 0.07$ and 9000 rpm is stable at high cavitation number, σ. It is also stable at low frequencies for all cavitation numbers. However, as σ is reduced the system becomes unstable in a cavitation number range of between 0.025 and 0.045; more transfer functions would have been needed to pinpoint the value more accurately. At least this covers the observed onset value of about 0.03 [5]. The figure also indicates instability above a reduced frequency of about 0.3 which is in accord with the results of Section 4.

Figure 13 presents similar results for Impeller 6. It shows a similarly decreasing Δe with frequency at higher frequencies when the cavitation number is decreased. However, the data of the transfer functions does not extend to a sufficiently high ω to yield negative Δe. The information is however fairly consistent with the observed onset at $\sigma \approx 0.05$ (see Figs. 6,7) at a reduced frequency in the range $0.55 \rightarrow 0.6$ (see Fig. 6)

Finally it is worth noting that the pump transfer function element whose change with cavitation number is primarily responsible for the trend toward negative Δe at higher frequencies has been shown in Ref. [5] to be the element ZP_{22}; that is to say, the

mass flow gain factor term. This is consistent with the analytical transfer functions derived using the bubbly-flow model (Ref. 23); the "active" dynamic characteristics in that model result from kinematic wave production in the neighborhood of inlet which primarily determine ZP_{22}.

9. CONCLUDING REMARKS

This paper has presented details of measurements on the instability known as auto-oscillation which occurs in systems with cavitating pumps. Specific measurements of onset cavitation number and auto-oscillation frequency are presented for a range of inducers; amplitude and phase information on various fluctuating pressures and flow rates have also been given. It has been demonstrated that auto-oscillation is a system instability caused by the active dynamic characteristics of the cavitating pump. A system analysis which uses previously measured transfer functions for the inducers as well as dynamic models for the remainder of the hydraulic system is investigated. Though this analysis does not yield results which are as decisive as one might wish, they are at least consistent with the observations in terms of the onset cavitation number and auto-oscillation frequency. Evidence is presented to show that the frequency (though not the onset) can be evaluated fairly accurately from estimates of the compliance and inertance of the pump which can be obtained directly from the pump transfer function as a function of cavitation number.

ACKNOWLEDGMENT

The authors would like to thank the NASA George Marshall Space Flight Center for their financial support under Contract NAS 8-29313, the National Science Foundation for support under Grant Eng. 76-11225, Professor A.J. Acosta for his inimitable insight during discussions and Edmund Lo, Greg Hoffman and Dan Rovner for help with the experiments.

REFERENCES

[1]. Abbot, H.F., Gibson, W.L., and McCaig, I.W., "Measurements of Auto-Oscillation in Hydroelectric Supply Tunnel and Penstock System", Jour. of Basic Eng. Vol. 85, 1963, pp. 625-630.

[2]. Acosta, A.J., "An Experimental Study of Cavitating Inducers", Proc. of 2nd O.N.R. Symp. on Nav. Hydro., August 25-29, 1958, (ACR-38).

[3]. Badowski, H.R., "An Explanation for Instability in Cavitating Inducers", ASME Cavitation Forum, 1969, pp. 38-40.

[4]. Barr, R.A., "Study of Instabilities in High Head Tandem Row Inducer Pumps", Hydronautics Interim Technical Report 703-1, February 1967.

[5]. Braisted, D.M., and Brennen, C., "Observations on Instabilities of Cavitating Inducers", ASME Cavitation Forum, 1978, pp. 19-22.

[6]. Etter, R.J., "An Investigation of Tandem Row High Head Pump Inducers", Hydronautics Technical Report 703-9, May 1970.

[7]. Kamijyo, K., Shimura, T., and Watanabe, M., "An Experimental Investigation of Cavitating Inducer Instability", ASME, 77-WA/FE-14, 1977.

[8]. Makhin, V.A., Gotsulenko, V.N. and Gotsulenko, N.N., "Instability (Surging) of Centrifugal Pump with Prepump", Soviet Aeronautics, Vol 18, No. 8, pp. 150-154, 1975.

[9]. Miller, C.D. and Gross, L.A., "A Performance Investigation of an Eight-Inch Hubless Pump Inducer in Water and Liquid Nitrogen", NASA TN D-3807, March 1967.

[10]. Natazon, M.S., Bal'Tsev, N.I., Bazhanov, V.V. and Leydervarger, M.R., "Experimental Investigation of Cavitation Induced Oscillations of Helical Inducers", Fluid Mechanics - Soviet Research, Vol. 3, No. 1, pp. 38-45, January-February 1974.

[11]. Ng. S.L., "Dynamic Response of Cavitating Turbomachines", Ph.D. Thesis, Calif. Inst. of Tech., Pasadena, Calif., 1976.

[12]. Ng, S.L., and Brennen, C., "Experiments on the Dynamic Behavior of Cavitating Pumps", Jour. of Fluids Eng. Vol. 100, pp. 166-176, June 1978.

[13]. Sack, L.E. and Nottage, H.B., "System Oscillations Associated with Cavitating Inducers", Jour. of Basic Eng., Vol. 87, pp. 917-924, 1965.

[14]. Young, W.E., Murphy, R. and Reddecliff, J.M., "Study of Cavitating Inducer Instabilities", PWA FR-5131, Pratt-Whitney Aircraft, August 1972.

[15]. Braisted, D.M., "Cavitation Induced Instabilities Associated with Turbo-machines", Ph.D. Thesis, Calif. Inst. of Tech., Sept. 1979.

[16]. Jaeger, C., "The Theory of Resonance in Hydropower Systems: Discussion of Incidents and Accidents Occurring in Pressure Systems", Jour. of Basic Eng. Trans., ASME, Vol. 85, pp. 631-640, 1963.

[17]. Brennen, C. "A Linear Dynamic Analysis of Vent Condensation Stability", submitted to the Jour. of Fluids Eng.

[18]. Rubin, S., "Longitudinal Instability of Liquid Rockets due to Propulsion Feedback (POGO)", Jour. of Spacecraft and Rockets, Vol. 3, No. 8, pp. 1188-1195, 1966.

[19]. Murphy, G.L., "POGO Suppression Analysis of the S-IT and S-IVB LOX Feed Systems", Report No. ASD-ASTN-1040, Brown Eng. Co., Huntsville, Ala. 1969.

[20]. Farrel, E.C. and Fenwick, J.R., "POGO Instabilities Suppression Evaluation", NASA Report CR-134500, 1973.

[21]. Brennen, C. and Acosta, A.J., "The Dynamic Transfer Function for a Cavitating Inducer", ASME, Jour. Fluids Eng., Vol. 98, pp. 182-191.

[22]. Brennen, C.E., Meissner,C., Lo, E.Y. and Hoffman, G.S., "Scale Effects in the Dynamic Transfer Functions for Cavitating Inducers". Submitted for publication.

[23]. Brennen, C., "Bubbly Flow Model for the Dynamic Characteristics of Cavitating Pumps", Jour. of Fluid Mech., Vol. 89, part 2, 1978, pp. 223-240.

[24]. Brennen, C., "The Unsteady, Dynamic Characterization of Hydraulic Systems with Emphasis on Cavitation and Turbomachines", Proc. Int'l. Ctr. for Heat & Mass Trans. 1978 Seminar in Dubrovnik, Yugoslavia.

[25]. Greitzer, E.M., "Surge and Rotating Stall in Axial Flow Compressors - Part I: Theoretical Compression System Model" and Part II: Experimental Results and Comparison with Theory", Jour. of Eng. for Power, Vol. 98, 1976, pp. 190-198 and 198-211.

[26]. Dean, R.C. and Young, L.R., "Time Domain of Centrifugal Compressor and Pump Stability and Surge", Jour. of Fluids Eng., Vol. 99, pp. 53-63, 1977.

[27]. Jackson, E.D., "Final Report Study of Pump Discharge Pressure Oscillations", Rocketdyne *Report No. R-6693-2, 1966.*

[28]. Rosenmann, W., "Mark 10 LOX Inducer Test Report", Internal Correspondence TAMM 2115-17, North American Aviation, February 28, 1962.

[29]. Rosenmann, W., "Model Mark 10 LOX Inducer Test Report", Internal Correspondence TAMM 4115-67, North American Aviation, June 11, 1964.

[30]. Acosta. A.J., and Wade, R.R., "Experimental Study of Cavitating Hydrofoils in Cascade", Final Report NASA Contract NGR 05-002,059, Feb. 1968.

[31]. Fanelli, M., "Further Considerations on the Dynamic Behavior of Hydraulic Turbo-machinery", Water Power, Vol. 24, No. 6, 1972, pp. 208-222.

[32]. Brown, F.T., "A Unified Approach to the Analysis of Uniform One-Dimensional Distributed Systems", Jour. of Basic Eng., Vol. 89, 1967, pp. 423-432.

[33]. Hennyey, Z., "Linear Electric Circuits", Pergamon Press, 1962.

[34]. Stepanoff, A.J., "Centrifugal and Axial Pumps; Theory, Design and Application", Wiley, 1948.

[35]. Streeter, V.L. and Wylie, E.B., "Hydraulic Transients", McGraw-Hill, 1967.

D. M. Braisted is now affiliated with the Exxon Production Research Company, Houston, Texas